

See discussions, stats, and author profiles for this publication at: <https://www.researchgate.net/publication/239717601>

Surface Reactions of Acetone on Al₂O₃, TiO₂, ZrO₂, and CeO₂: IR Spectroscopic Assessment of Impacts of the Surface Acid–Base Properties

ARTICLE *in* LANGMUIR · JANUARY 2001

Impact Factor: 4.46 · DOI: 10.1021/la000976p

CITATIONS

76

READS

91

3 AUTHORS, INCLUDING:



Mohamed I Zaki

Minia University

188 PUBLICATIONS 3,618 CITATIONS

SEE PROFILE

Surface Reactions of Acetone on Al_2O_3 , TiO_2 , ZrO_2 , and CeO_2 : IR Spectroscopic Assessment of Impacts of the Surface Acid–Base Properties

M. I. Zaki,* M. A. Hasan, and L. Pasupulety

Chemistry Department, Faculty of Science, Kuwait University, P.O. Box 5969
Safat, 13060 Kuwait

Received July 11, 2000. In Final Form: November 7, 2000

Adsorption and surface reactions of acetone vapor were observed on the title oxides at room and higher temperatures (up to 400 °C), using in situ infrared spectroscopy. The results were correlated with results of infrared spectroscopy of adsorbed pyridine, to assess impacts of the surface acid–base properties. It was found that the availability of Lewis acid sites is essential for anchoring acetone molecules to the surface. Coexisting Lewis base sites catalyze condensation of the acetone molecules into mesityl oxide surface species, via formation and subsequent decomposition of enolate and diacetone alcohol species. When intimately coupled, the Lewis acid and base sites generate pair sites of particularly strong adsorption capacity toward condensation products thus formed. Consequently, surface active sites are blocked and adsorptive and catalytic interactions of acetone are largely suppressed.

Introduction

Surface chemistry of acetone has been the focus of attention of a number of recent research endeavors.^{1–4} The thrust for this research interest has been the knowledge that catalytic hydrogenation of acetone is a versatile synthetic route to fine chemicals.^{5–7} Among the products encountered are the industrially important 4-hydroxy-4-methylpentan-2-one, methyl isobutyl ketone (MIBK), diacetone alcohol (DAA), and mesityl oxide (MSO).^{6,7} Hydrogenation of acetone has been found to occur on metal-oxide-supported Ni, Co, and Fe metal catalysts^{5–7} at low temperatures (150–250 °C), near atmospheric pressure.

Studies conducted to understand the surface chemistry of acetone were based largely on in situ IR probing of adsorption modes and species of acetone on metal oxide surfaces at low^{1,2} and high^{3,4} temperatures. The results obtained may lead to the following conclusions. First, acetone molecules are irreversibly adsorbed via coordination to Lewis acid sites ($(\text{CH}_3)_2\text{C}=\text{O} \rightarrow \text{M}^{n+}$). Second, the acetone ligands may be activated for α -hydrogen abstraction and consequent formation of anionic enolate-type ions ($\text{CH}_2(\text{CH}_3)\text{C}=\text{O} \rightarrow \text{M}^{n+}$), provided that the coordination site is strongly acidic and has a basic site (surface $-\text{OH}^-$ or $-\text{O}^{2-}$ site) in close proximity. Third, an aldol-condensation-type of surface reaction may then occur, converting the enolate species into DAA ($(\text{CH}_3)_2\text{C}(\text{OH})\text{CH}_2(\text{CH}_3)\text{C}=\text{O} \rightarrow \text{M}^{n+}$) and further to MSO ($(\text{CH}_3)_2\text{C}=\text{CH}-(\text{CH}_3)\text{C}=\text{O} \rightarrow \text{M}^{n+}$) species. Fourth, occurrence of aldol condensation implies, according to the reaction mechanism published elsewhere,⁸ the availability on the

surface of acid–base site-pairs functioning in a concerted fashion. Last of all, acetone adsorbed species are converted at high temperatures (>200 °C) into acetate surface species. It is obvious from these conclusions that surface reactions of acetone are critically controlled by the acid–base properties of the surface.

In an attempt to correlate catalysis-induced changes in the chemical composition of the acetone gas phase with the type of adsorbed acetone species, Fouad et al.⁹ suggested that strong adsorption of the primary (coordinated) species and/or condensation (polymerized) products of acetone blocks the active sites for further adsorptive and catalytic interaction. This suggestion was based on observed decomposition reactions of methylbutynol (giving “acetone + acetylene”) that slow markedly on surfaces (Y^{3+} -doped MgO) exposing strong acid–base site-pairs, known to facilitate strong adsorption and subsequent condensation of the acetone thus produced. These authors⁹ stressed that such aldol-condensation-type reactions require not only basic sites at which C–H bond activation takes place⁸ but also coexisting Lewis acid sites to stabilize the reaction intermediates. This was verified earlier by blocking the Lewis acid sites via adsorption of pyridine.¹⁰

Acetone produced via 2-propanol dehydrogenation on group IVB metal oxides was found to convert to isobutene and CH_4 gas-phase products at 300–400 °C, without any sign of formation of acetone condensation products on the surface.^{11,12} Whether that was due to involvement of Lewis acid sites in coordinating isopropoxide species (or the simultaneously formed acetate species), leading to the absence on the test surfaces of cooperatively functioning acid–base site-pairs, is a question that could find no definitive answer by the results then communicated.^{11,12} As a matter of fact, dehydrogenation of

* Corresponding author. E-mail: zaki@kuc01.kuniv.edu.kw. Fax: (0965)4846946.

(1) Allian, M.; Borello, E.; Ugliengo, P.; Spanò, G.; Garrone, E. *Langmuir* **1995**, *11*, 4811.

(2) Panov, A.; Fripiat, J. J. *Langmuir* **1998**, *14*, 3788.

(3) Fouad, N. E.; Thomasson, P.; Knözinger, H. *Appl. Catal., A* **2000**, *196*, 125.

(4) Zaki, M. I.; Hasan, M. A.; Al-Sagheer, L.; Pasupulety, L. *Langmuir* **2000**, *16*, 460.

(5) Gandia, L.; Montes, M. *Appl. Catal., A* **1993**, *101*, L1.

(6) Narayanan, S.; Unnikrishnan, R. *Appl. Catal., A* **1996**, *145*, 231.

(7) Narayanan, S.; Unnikrishnan, R. *J. Chem. Soc., Faraday Trans.* **1998**, *94*, 1123.

(8) Iglesia, E.; Barton, D. G.; Biscardi, J. A.; Gines, M. J. L.; Soled, S. L. *Catal. Today* **1997**, *38*, 339.

(9) Fouad, N. E.; Thomasson, P.; Knözinger, H. *Appl. Catal., A* **2000**, *194–195*, 213.

(10) Tanabe, K.; Saito, K. *J. Catal.* **1974**, *35*, 247.

(11) Zaki, M. I.; Hussein, G. A. M.; El-Ammawy, H. A.; Mansour, S. A. A.; Poltz, J.; Knözinger, H. *J. Mol. Catal.* **1990**, *57*, 367.

(12) Hussein, G. A. M.; Sheppard, N.; Zaki, M. I.; Fahim, R. B. J. *Chem. Soc., Faraday Trans. 1* **1989**, *85*, 1723.

Table 1. IR/Py-Probed Surface Acid and Base Sites on the Test Oxides

oxide	Py adsorbed species ^a	characteristic IR frequency/ ± 2 cm ⁻¹	thermal stability/ $^{\circ}$ C	surface acid site	surface base site	supporting reference
Al	LPy	1622	≤ 300	Al ³⁺ (t) ^b		15, 17, 18
		1612	< 300	Al ³⁺ (o) ^c		15, 17, 18
	HPy	1596	< 200	OH ^{d+}		15, 17, 18
Ti	LPy(C=O)	1680 ^d	> 300		OH ⁻	15, 17
	LPy	1633 ^e	≤ 300	Ti ⁴⁺ (a) ^f		15, 12
		1605	< 300	Ti ⁴⁺ (r) ^g		15
Zr	HPy	1594	≤ 200	OH ^{d+}		15, 12
	BPy	1650 ^h	≤ 200	OH ⁺		15
	LPy	1605	≤ 200	Zr ⁴⁺		15, 12
Ce	HPy	1588	≤ 200	OH ^{d+}		15, 12
	LPy(C=O)	1675 ^d	≥ 300		OH ⁻	15
	LPy	1618	< 200	Ce ⁴⁺		15, 19
		1595	< 200	OH ^{d+}		15, 19
	LPy(C=O)	1670	≥ 200		OH ⁻	15, 19
	LPy(N ⁺ -O)	1270 ⁱ	≥ 200		O ²⁻	15, 19, 20

^a LPy, Py coordinated to Lewis acid sites; HPy, H-bonded Py; BPy, protonated Py via Bronsted acid sites; LPy(C=O), coordinated α -pyridone; LPy(N⁺-O), coordinated pyridinium oxide. ^b Tetrahedrally coordinated Al³⁺. ^c Octahedrally coordinated Al³⁺. ^d Resolved from nearby δ H₂O contribution. ^e Occurring in the absence of ν 19b absorption at 1550–1530 cm⁻¹. ^f Contained in anatase-structured TiO₂. ^g Contained in rutile-structured TiO₂. ^h Occurring in the presence of ν 19b absorption at 1550 cm⁻¹. ⁱ Occurring together with two absorptions at 1160 and 1090 cm⁻¹.

2-propanol cannot exclusively indicate availability of strong basic sites (e.g., O²⁻ sites) on the catalytic surface,¹³ because redox sites (e.g., Mⁿ⁺/M⁽ⁿ⁻¹⁾⁺) may also catalyze alcohol dehydrogenation.¹⁴

The present investigation was designed to assess impacts of the surface acid–base properties on adsorptive and catalytic interactions of acetone. To accomplish this objective, (i) a number of metal oxides (Al₂O₃, TiO₂, ZrO₂, and CeO₂) of varied acid–base properties¹⁵ were selected to provide the test surfaces, (ii) pyridine adsorption was used to probe the surface acid–base properties,¹⁵ (iii) both surface and gas-phase species of acetone/oxide were determined as a function of temperature (room temperature (RT)–400 $^{\circ}$ C) in near-equilibrium conditions, and (iv) in situ IR spectroscopy was employed to examine the gas/solid interface.

Experimental Section

Metal Oxides. Test metal oxides were $\sim 99\%$ pure Degussa Aluminumoxide C ($(\gamma + \delta)$ -Al₂O₃, 107 m²/g) and P25 titania (anatase TiO₂, 50 m²/g), MEL zirconia (monoclinic + tetragonal) ZrO₂, 34 m²/g), and Rhône-Poulenc ceria (fluorite CeO₂, 31 m²/g). For simplicity, they are denoted as Al, Ti, Zr, and Ce, respectively. These oxides were used as provided.

Adsorptives and Gases. Adsorptive molecules were provided by expanded vapors of liquid acetone (denoted Ac) and pyridine (Py) at RT; their source liquids being AR-grade products of BDH. They were deaerated prior to application, by on-line freeze–pump–thaw cycles performed at liquid nitrogen temperature (-195 $^{\circ}$ C). N₂ and O₂ gases were 99.999% pure products of KOAC (Kuwait) and were used as supplied. The former gas was the adsorptive used for surface area measurements (vide supra), whereas the latter was used to burn off surface impurities in the in situ pretreatment of oxide wafers used for IR measurements (vide infra).

In Situ IR Spectroscopy. A heatable and evacuable, all-Pyrex glass IR cell equipped with CaF₂ windows as described earlier¹⁶ was used to facilitate examination of both gas-phase and adsorbed species produced as a result of Ac surface reactions (at RT–400 $^{\circ}$ C) on the test metal oxides. It was also used to

identify adsorbed species of pyridine (at RT–400 $^{\circ}$ C) on the same test oxides. A model Spectrum-BX FTIR Perkin-Elmer was the spectrometer employed. The sample compartment was purged with dry N₂ for 10 min prior to recording the spectra. A background spectrum was taken of the oxide mounted inside the cell in the form of a thin self-supporting wafer, following a high-temperature treatment in O₂ atmosphere, subsequent outgassing to 10^{-6} Torr and cooling to RT, as described earlier.⁴ This spectrum was used to probe the surface atomic groups and impurity species before exposure to the adsorptive atmosphere. Then, a 10-Torr portion of Ac vapor was admitted into the cell and kept for 5 min in contact with the oxide wafer at the desired temperature, followed by cooling to RT. A spectrum of the “gas phase + oxide” and another of the “gas phase” only (the wafer was lifted out of the optical path) were recorded. (A third spectrum of the “oxide” only was also recorded after outgassing for 5 min.) A fresh 10-Torr portion of Ac vapor was used for each adsorption/reaction temperature. In the case of Py, the oxide wafer was exposed to 2–3 Torr of Py vapor for 5 min at the desired adsorption temperature (RT–400 $^{\circ}$ C), cooled to RT, and outgassed for 5 min, and a spectrum was taken of the oxide only. Difference spectra of the gas-phase and adsorbed species were obtained by absorption subtraction of the appropriate spectra, using P-E Spectrum version 2.0 software. These procedures and measurements were described in detail previously.⁴

Results and Discussion

Surface Acid–Base Properties. Table 1 summarizes results monitored by IR spectra of Py adsorbed on the test oxides as a function of temperature (RT–400 $^{\circ}$ C).¹⁵ It is obvious that Lewis acid sites (L-sites) and H-bond donor sites are found on all of the test oxides. The former type of site is associated with coordinatively unsaturated (cus) metal ions,^{21,22} whereas the latter type is related to partially positively charged surface OH groups.¹⁸ Provided that the higher the ν 8a frequency of the ring breathing vibrations (ν CCN vibrations) of LPy species (Py coordinated to L-sites) the stronger the associated Lewis acid site,²³ the relatively strongest Lewis acid sites are those (cus Ti⁴⁺) exhibited on anatase-structured TiO₂. On the

(13) Lahousse, C.; Bachelier, J.; Lavalley, J. C.; Lauron-Pernot, H.; Le Govic, A. M. *J. Catal.* **1994**, *87*, 537.

(14) Nondek, L.; Sedlack, J. *J. Catal.* **1975**, *40*, 34. Nondek, L.; Kraus, M. *J. Catal.* **1975**, *40*, 40.

(15) Zaki, M. I.; Hasan, M. A.; Al-Sagheer, F. A.; Pasupulety, L. *Colloids Surf., A*, submitted.

(16) Peri, J. B.; Hannan, R. B. *J. Phys. Chem.* **1960**, *64*, 1526.

(17) Boehm, H.-P.; Knözinger, H. In *Catalysis-Science and Technology*; Anderson, J. R., Boudart, M., Eds.; Springer-Verlag: Berlin, 1983; Vol. 4, pp 39–207.

(18) Zaki, M. I.; Knözinger, H. *Mater. Chem. Phys.* **1987**, *17*, 201.

(19) Zaki, M. I.; Hussein, G. A. M.; Mansour, S. A. A.; El-Ammawy, H. A. *J. Mol. Catal.* **1989**, *51*, 209.

(20) Urban, M. W. *Vibrational Spectroscopy of Molecules and Macromolecules on Surfaces*; J. Wiley & Sons: Chichester, 1993; pp 171–185.

(21) Farragher, A. L. *Adv. Colloid Interface Sci.* **1979**, *11*, 3.

(22) Knözinger, H. In *Surface Organometallic Chemistry: Molecular Approaches to Surface Catalysis*; Basset, J.-M. et al., Eds.; Kluwer Academic Publ.: New York, 1988; pp 35–46.

other hand, most of the H-bond donating OH groups have been found¹⁵ to be either bridging or multicentered groups. The surface of Zr is shown to be unique in exposing Brønsted acid sites (B-sites), as identified by the formation of BPy species (protonated Py, Table 1). Ti appears to be distinct by the absence on its surface of detectable basic sites (neither OH⁻ nor O²⁻). In contrast, Ce exposes both OH⁻ and O²⁻ basic sites, whereas Al and Zr exhibit the former type of basic site only. However, Al may expose O²⁻ sites following an effective dehydroxylation.¹⁸

The conversion of LPy species into LPy(C=O) species (α -pyridone) at high temperatures implies the presence of basic OH groups,¹⁷ whereas the conversion into LPy-(N⁺-O) (pyridinium oxide) species is considered to be indicative of basic O²⁻ sites.^{19,24} According to Boehm and Knözinger,¹⁷ high-temperature interactions leading to selective oxidation of LPy species must be preceded by sufficient activation of the Py ligands for the nucleophilic attack. Thus, LPy oxidation would require availability not only of basic sites but also of strong L-sites functioning in a concerted mechanism with the basic sites. The results shown in Table 1 can, therefore, account for the presence of acid-base site-pairs on Ce, Al, and Ti, being relatively more obvious on Ce. Adsorbed Py was deeply oxidized at a temperature as low as 200 °C on Ce surfaces. The products were carboxylate, carbonate, and NO_x surface species. Similar results were observed previously.^{19,25} These results have been considered indicative of the uniquely high strength and reactivity of basic sites on Ce surfaces.^{15,19,25}

IR Spectra of Adsorbed Acetone at RT. Figure 1 compares the IR spectrum taken at 1800–1200 cm⁻¹ (ν C=O/C=C/ δ CH region) of acetone irreversibly adsorbed on alumina (Ac/Al) at RT and spectra taken of gas-phase acetone (Ac) and mesityl oxide (MSO), also at RT. MSO is often the eventual product of aldol-condensation-like surface reactions of Ac,⁸ as manifested in Figure 2A. It is obvious from the gas-phase spectra that MSO is distinguishable from Ac by the ν C=C band at 1634 cm⁻¹. Moreover, the ν C=O and ν C-C bands of MSO occur at detectably lower (1707 vs 1740 cm⁻¹) and higher (1294 vs 1218 cm⁻¹) frequencies, respectively, than those of Ac. It has earlier been shown⁴ that in the liquid phase (stronger intermolecular interactions), the C=O and C=C stretching frequencies of both Ac and MSO are red-shifted to occur at 1690 and 1620 cm⁻¹, respectively. The same applies to the ν C-C of MSO, which has been found⁴ to occur at 1220 cm⁻¹ for the liquid phase. Literature IR spectral data found for Ac and MSO molecules coordinated to surface L-sites are summarized in Figure 2B. Figure 2B also summarizes similar data for the intermediate enolate (ENOL) and DAA formed throughout the condensation of Ac into MSO (Figure 2A). The data depicted in Figure 2B are only for the diagnostic frequencies of each of these materials in the adsorbed state.

The IR spectrum taken of Ac/Al (Figure 1) displays a strong absorption at 1702 cm⁻¹, a shoulder at 1675 cm⁻¹, a composite absorption centered around 1611 cm⁻¹, two weak absorptions at 1451 and 1422 cm⁻¹, and two moderate absorptions at 1370 and 1236 cm⁻¹. According to the reference data shown in Figure 2B, the absorptions at 1702–1611 cm⁻¹ are assignable to ν C=O of Ac coordinated to weak (1702 cm⁻¹) and strong (1675 cm⁻¹)

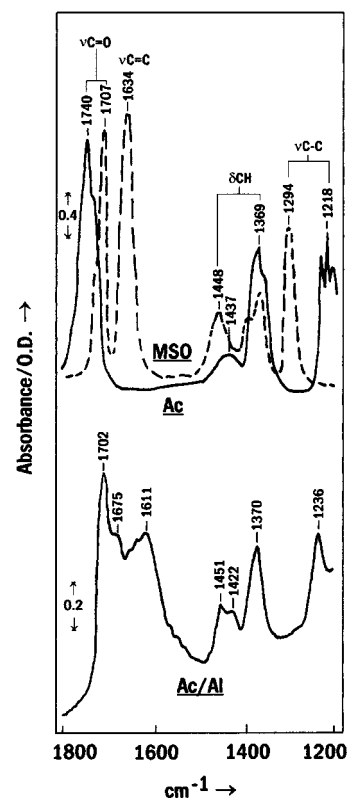


Figure 1. IR spectra taken of 10 Torr of gas-phase acetone (Ac) and mesityl oxide (MSO) and of irreversibly adsorbed acetone on alumina (Ac/Al) at RT.

L-sites and ν C=O of coordinated MSO and/or DAA species (1611 cm⁻¹). The absorptions at 1451–1236 cm⁻¹ can, accordingly, be assigned to ν CH (1451–1370 cm⁻¹) and ν C-C (1236 cm⁻¹) vibrations of Ac, MSO, and/or DAA adsorbed species. Because formation of DAA or MSO species may mark involvement of adsorbed Ac in aldol-condensation-like reactions (Figure 2A), an absorption due to the diagnostic ν C \equiv C \cdots O⁻ vibrations (at 1575–1525 cm⁻¹)^{26,27} of the intermediate ENOL species can still be included in the band structure exhibited. The reaction pathways depicted in Figure 2A may imply the availability of the necessary acid and base sites on Al surfaces. The Py-probed acid-base properties of Al (Table 1) indicate consistently the availability on Al of two types of L-sites, viz., octahedral and tetrahedral cus Al^{3+} , and both H-bond donor and basic OH groups. According to Knözinger and Ratnasamy²⁸ as well as Nortier et al.,²⁹ different types of isolated surface OH groups of varied acid-base properties are exposed on γ -Al₂O₃: basic Al-OH's and acidic (Al)_xOH's. Strong Lewis base O²⁻ sites are not produced on Al unless the surface is effectively dehydroxylated ($2^-\text{OH-surf} \rightarrow \text{O}^{2-}\text{-surf} + \text{H}_2\text{O}$)²⁸ via prolonged thermoevacuation at temperatures well above 900 °C.³⁰

The spectrum exhibited by Ac/Al at RT is compared in Figure 3 with analogous spectra exhibited by irreversibly adsorbed Ac on Ti, Zr, and Ce, also at RT. Figure 3B displays the spectra measured over the ν C=O/C=C/C-C/ δ CH range of frequency (1800–1200 cm⁻¹), whereas

(23) Paukshtis, E. A.; Yurchenko, E. N. *Russ. Chem. Rev. (Engl. Transl.)* **1983**, 52, 242.

(24) Niwa, M.; Furukawa, Y.; Murakami, Y. *J. Colloid Interface Sci.* **1982**, 86, 260.

(25) Binet, C.; Badri, A.; Boutonnet-Kizling, M.; Lavalley, J. C. *J. Chem. Soc., Faraday Trans.* **1994**, 90, 1023.

(26) Miyata, H.; Toda, Y.; Kubokawa, Y. *J. Catal.* **1974**, 32, 155.

(27) Busca, G.; Lorenzelli, V. *J. Chem. Soc., Faraday Trans. 1* **1982**, 78, 2911.

(28) Knözinger, H.; Ratnasamy, P. *Catal. Rev.—Sci. Eng.* **1978**, 17, 31.

(29) Nortier, P.; Fourre, P.; Saad, A. B. M.; Saur, O.; Lavalley, J. C. *Appl. Catal.* **1990**, 61, 141.

(30) Ballinger, T. H.; Yates, J. T., Jr. *Langmuir* **1991**, 7, 3041.

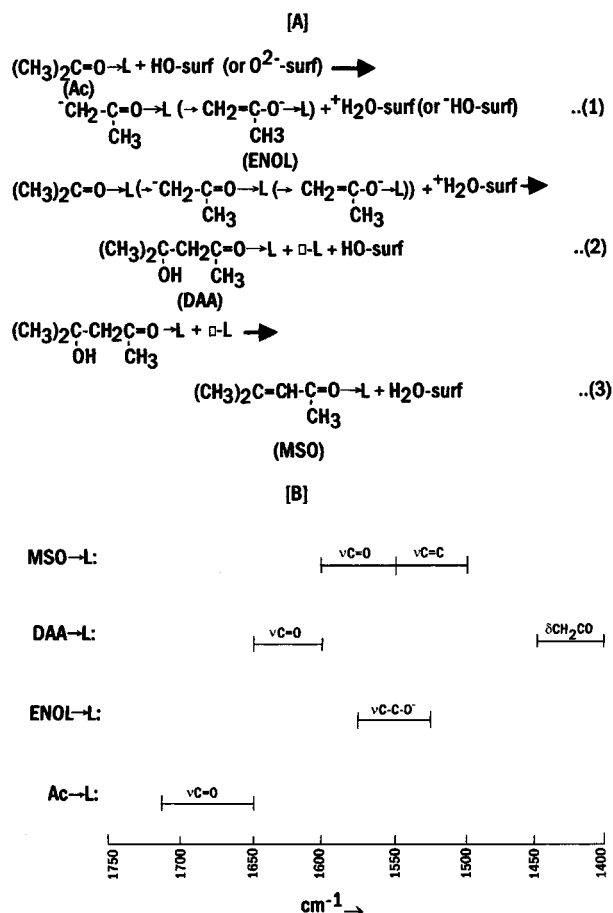


Figure 2. Literature data found for pathways of aldol-condensation-like surface reactions [A]^{4,8} and IR diagnostic frequencies of adsorbed reaction products [B] (refs 2, 4, and 26).

spectra recorded over the νCH range of frequency ($3100\text{--}2500\text{ cm}^{-1}$) are exhibited in Figure 3A. It is obvious from Figure 3B that the spectra taken of Ac/Zr and Ac/Ce monitor two notably different band structures. On the other hand, those of Ac/Al and Ac/Ti display composite band structures made, apparently, out of mixed spectral features of the former two band structures. Hence, the spectra of Ac/Zr and Ac/Ce may be considered indicative of the dominance of two different adsorbed species each established on either of the two test oxides. The well-defined IR absorptions displayed in the spectrum of Ac/Zr maximize at frequencies (1703 , 1367 , and 1229 cm^{-1}) very close to those assignable to $\nu\text{C}=\text{O}$ (1711 cm^{-1}), δCH (1368 cm^{-1}), and $\nu\text{C}-\text{C}$ (1230 cm^{-1}) of Ac molecules coordinated to L-sites²⁻⁴ ($\text{Ac} \rightarrow \text{Zr}^{4+}$). The weak bands at 1467 and 1422 cm^{-1} are due also to δCH vibrations. The latter band probably originates from the $\text{Ac} \rightarrow \text{L}$ species,^{2,4} and the former from a different Ac interaction species. The weak, broad shoulder centered around 1620 cm^{-1} is due to $\nu\text{C}=\text{O}$ vibrations originating from minority condensation species of adsorbed Ac and/or minority Ac molecules coordinated to stronger L-sites (i.e., more coordinatively unsaturated Zr^{4+} sites). The corresponding νCH spectrum (Figure 3A) displays two absorptions at 2962 and 2931 cm^{-1} and three shoulders at 3005 , 2869 , and 2815 cm^{-1} for Ac/Zr at RT. These νCH absorptions are closer to those of liquid-phase^{4,31} than gas-phase⁴ Ac and may shroud contributions from the minority condensation species of adsorbed acetone molecules.

(31) *Merck FT-IR Atlas*; Pachler, K. G. R., Matlok, F., Gremlich, H.-U., Eds.; VCH: Weinheim, 1988.

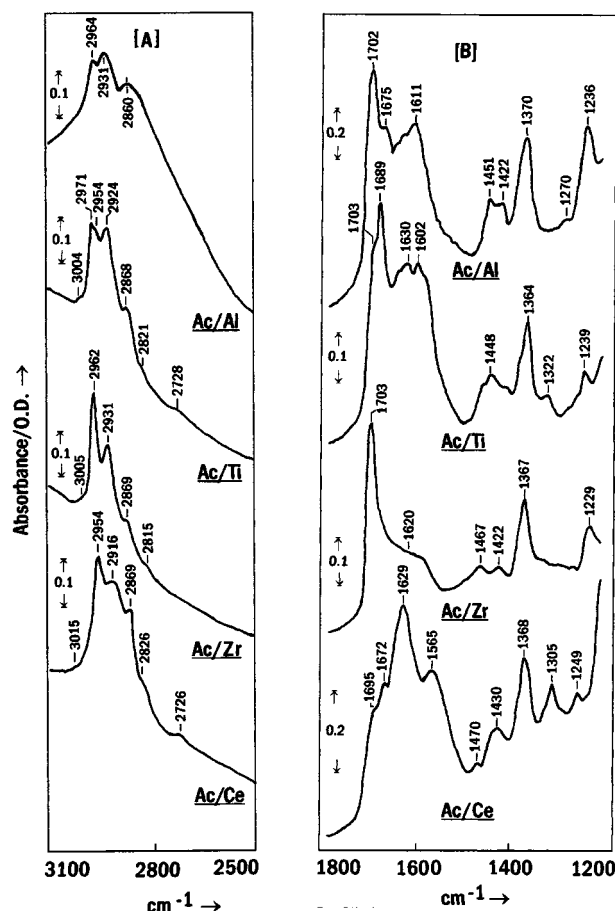


Figure 3. IR νCH [A] and $\nu\text{C}=\text{O}/\text{C}=\text{C}/\text{C}-\delta\text{CH}$ [B] spectra taken of reversibly adsorbed acetone (Ac) on the oxides indicated at RT.

On the other hand, the spectrum of Ac/Ce (Figure 3B) exhibits a rather strong, broad absorption at $\geq 1500\text{ cm}^{-1}$ resolving four maxima at 1695 , 1672 , 1629 , and 1565 cm^{-1} . According to the frequency classification manifested in Figure 2B, the former two maxima are most likely due to Ac molecules coordinated to two different types of L-sites (Ce^{4+} sites). On the other hand, the latter two maxima are most probably associated with Ac condensation species. Furthermore, the weak absorption displayed (Figure 3B) at 1430 cm^{-1} is most likely assignable to δCH vibrations in $-\text{CH}_2-\text{C}=\text{O}$ groups of DAA-like species. This δCH absorption, together with the $\nu\text{C}=\text{O}$ absorption at 1629 cm^{-1} , may imply formation of DAA→L species. The remaining $\nu\text{C}=\text{O}$ absorption occurs at a much lower frequency (1565 cm^{-1}) than would be expected for $\text{Ac} \rightarrow \text{L}$ species.^{2,4} Figure 2B may help in ascribing it to MSO→L species. However, its notable broadness may also include a contribution from $\nu\text{C}-\text{C}-\text{O}^-$ vibrations of ENOL→L species. The expected $\nu\text{C}=\text{C}$ frequency ($1550\text{--}1500\text{ cm}^{-1}$)^{2,3} of MSO may be shrouded by the strong $\nu\text{C}=\text{O}$ absorption, whereas the expected olefinic νCH absorption may be that resolved in the corresponding spectrum (Figure 3A) at 3015 cm^{-1} .^{3,9} The νCH absorptions at 2916 and 2726 cm^{-1} can lend further support to the formation of MSO→L species. The two weak absorptions resolved in the $\delta\text{CH}/\nu\text{C}-\text{C}$ region of the spectrum of Ac/Ce (Figure 3B) do not belong to $\text{Ac} \rightarrow \text{L}$ species. They may thus relate to coordinated DAA and MSO species. What is obvious from the spectra of Ac/Ce is that condensation species of Ac are more dominant than the primary ($\text{Ac} \rightarrow \text{L}$) species on Ce surfaces. Therefore, Ac/Ce may be considered the opposite

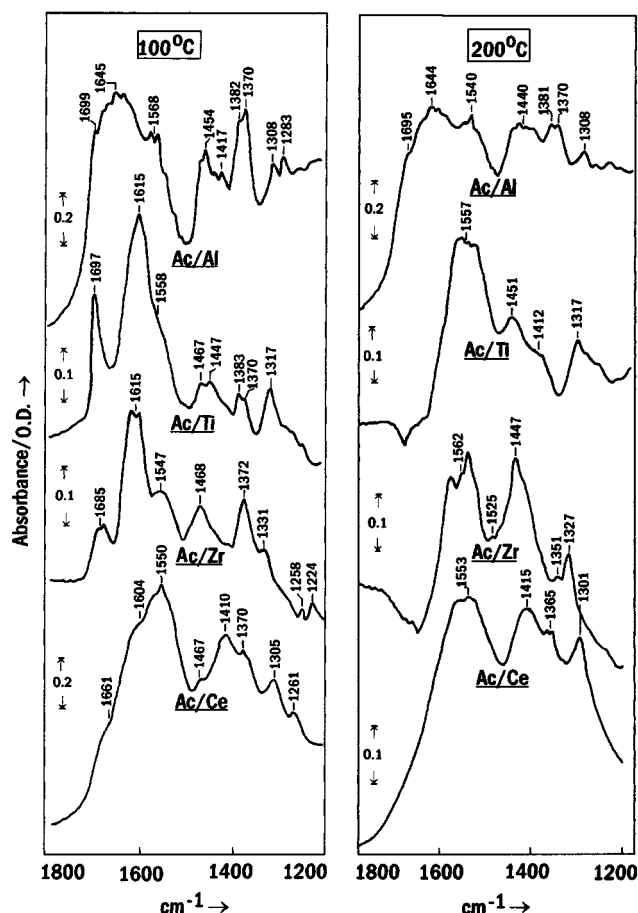


Figure 4. IR $\nu\text{C}=\text{O}/\text{C}=\text{C}/\text{C}-\text{C}/\delta\text{CH}$ spectra taken of irreversibly adsorbed species following exposure of test oxides to acetone (Ac) vapor at 100 °C [A] and 200 °C [B].

extreme of Ac/Zr, which is dominated by the primary (coordinated) species of Ac molecules (Figure 3B).

As mentioned above, the spectra taken of Ac/Al and Ac/Ti (Figure 3) monitor composite band structures consisting of mixed spectral features similar to those monitored in the spectra of Ac/Zr and Ac/Ce. The former spectra monitor various absorptions implying formation of primary (Ac \rightarrow L) and condensation (ENOL, DAA, and MSO) species of adsorbed Ac. It appears from the relative intensities of the various $\nu\text{C}=\text{O}$ absorptions (1703–1500 cm^{-1}) that the primary species are slightly more abundant than the condensation species of Ac on both Al and Ti. This may also be inferred from the corresponding νCH spectra shown in Figure 3A, particularly for Ac/Al. Thus, the RT adsorptive behavior of Ac molecules on Al and Ti appears to be intermediate between the two extreme behaviors shown by Ac/Zr (dominance of primary species) and Ac/Ce (dominance of condensation species).

IR Spectra of Adsorbed Acetone at $>\text{RT}$. IR spectra were taken at RT following adsorption of acetone on the test oxides at 100–400 °C. The spectra exhibited by adsorbed acetone at 100 and 200 °C are compared in parts A and B of Figure 4, respectively. It is obvious that at 100 °C absorptions due to $\nu\text{C}=\text{O}$ (at $\geq 1650 \text{ cm}^{-1}$) of primary Ac \rightarrow L species are partially suppressed on Al and Ti but considerably suppressed on Zr and Ce. They are replaced by enforced absorptions assignable to DAA ($\nu\text{C}=\text{O}$ at 1650–1600 cm^{-1}) and MSO ($\nu\text{C}=\text{O}$ at 1600–1550 cm^{-1}) species. DAA \rightarrow L appears to be the major species on Al, Ti, and Zr. In contrast, MSO \rightarrow L is implied to be the major species on Ce. The abundance of DAA species is shown (Figure 4A) by the sustenance of IR absorption in the δCH

frequency region (at 1450–1400 cm^{-1}), resulting from its $-\text{CH}_2-\text{C}=\text{O}$ groups, whereas the abundance of MSO species on Ce is accompanied by IR absorptions at 1550–1500 (ill resolved) and 3020–3010 cm^{-1} (not shown), resulting from $\nu\text{C}=\text{C}$ and olefinic νCH vibrations, respectively. The shoulders displayed at 1661 and 1604 cm^{-1} in the spectra of Ac/Ce may account for minority Ac \rightarrow L and DAA species, respectively, whereas the shoulders observed at 1568–1547 cm^{-1} in the spectra of acetone adsorbed on Al, Ti, and Zr may relate to minority MSO species.

At the higher temperature of 200 °C, the spectra obtained (Figure 4B) do not clearly monitor spectral features of the primary Ac \rightarrow L species, except on Al where the shoulder resolved at 1695 cm^{-1} is due most likely to its $\nu\text{C}=\text{O}$ vibrations. The spectra are generally dominated by two strong, broad absorptions at 1562–1540 and 1451–1415 cm^{-1} . The former absorption most likely owes much of its intensity to $\nu\text{C}=\text{O}$ vibrations of MSO species, though some contribution from the carbonyl group of DAA species (Figure 2B) cannot be ruled out. The $\nu\text{C}=\text{C}$ vibrations of MSO, expected to occur at 1550–1500 cm^{-1} , can still be accommodated in the absorption range of the former band. The latter band (1451–1415 cm^{-1}) is due most likely to δCH vibrations in $-\text{CH}_2-\text{C}=\text{O}$ and/or $-\text{CH}_2-$ groups, thus emphasizing the occurrence of MSO species without exclusion of coexisting DAA species. Spectra taken (at RT) following Ac adsorption on the various test oxides at ≥ 300 °C were rather similar in monitoring nothing but two strong, analogous absorptions, occurring, however, at higher frequency ranges: 1575–1566 and 1480–1468 cm^{-1} . It has been well established that two absorptions in these frequency ranges originating from high-temperature adsorption of hydrocarbons or organic oxygenates on metal oxide surfaces are due to νCOO^- vibrations of surface acetates.^{4,12,17} Though the present results cannot exclude some contribution from surface acetates to the present two 200 °C bands (Figure 4B), their seemingly lower frequency ranges may attribute much of their occurrence to condensation species (mostly MSO) of adsorbed Ac. A similar reasoning has been adopted recently by Fouad et al.,^{3,9} so as to attribute IR bands at 1585, 1523, and 1453 cm^{-1} solely to formation of MSO species during adsorption of Ac on MgO and Y/MgO at 200 °C.

IR Spectra of Acetone Gas Phase. IR spectra were taken of a 10-Torr portion of gas-phase Ac as a function of temperature (RT–400 °C), in absence and presence of the test oxides. The spectra obtained in absence of the oxides verified the stability of Ac to heating to 400 °C. They showed nothing but the characteristic absorptions of acetone molecules in the gas phase (Figure 1), thus excluding formation of pyrolytic products of Ac at any detectable level.

In presence of the test oxides, the temperature effects on the Ac gas phase were different depending on the temperature regime applied and the oxide used. At the low-temperature regime of RT–200 °C, the spectra indicated 8–32% consumption of the Ac gas phase depending on the oxide mounted. This consumption was not compensated for by release of products into the gas phase. Thus, it may be attributed only to noncatalytic adsorptive interactions of Ac molecules. When heating was done at the elevated temperatures of 300–400 °C, the consumption of the Ac gas phase increased to 42–83% (depending on the oxide tested) and products consisting of propene, methane, and CO_2 were observed in the gas phase. These products are not expected to result from condensation of Ac molecules.⁸ Results of a separate

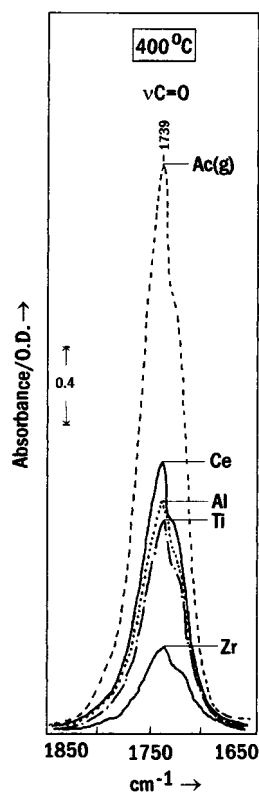


Figure 5. IR $\nu\text{C}=\text{O}$ absorption of acetone molecules in the gas phase recorded at RT following heating to 400 °C in presence of the oxides indicated.

investigation being performed in this laboratory could ascribe the acetone conversion into propene, methane, and CO_2 to reactions catalyzed essentially by Lewis and Brønsted acid sites exposed on oxide surfaces. These results will be communicated shortly.³² Accordingly, the catalytic activity observed at 300–400 °C cannot be related to the aldol-condensation-type of surface reactions observed for Ac on the test oxides.

Quantitation of Ac molecules in the gas phase was based on a peak area calculation for the $\nu\text{C}=\text{O}$ absorption at 1739 cm^{-1} . The peak area changes observed at 400 °C as a function of the oxide mounted are exhibited in Figure 5. They are further manifested (Figure 6) over the νCH region (3200–2500 cm^{-1}) in gas-phase spectra obtained at 200 and 400 °C. Formation of propene (P) was diagnosed by the two absorptions indicated (3079 and 2945 cm^{-1}) as well as a sharp absorption at 890 cm^{-1} .³³ Formation of methane (M) is indicated by a sharp absorption at 1305 cm^{-1} in addition to that (3016 cm^{-1}) shown in Figure 6.³³ On the other hand, CO_2 was identified by its antisymmetric νCO stretching vibration at 2348 cm^{-1} .³³ According to the quantitative data determined at 400 °C (Figure 6), the oxide activity toward Ac conversion (or consumption) can be ranked in the following descending order: $\text{Zr} > \text{Ti} \approx \text{Al} > \text{Ce}$. This order of decreasing activity parallels the increase in the surface basicity (Table 1). Thus, the highest activity observed for Zr (83% conversion) may be due to the availability on its surface of catalytic acid sites in the absence of detectable basic sites (Table 1). On the other hand, the lowest activity shown by Ce (42% conversion) may be related to the availability on its surface of strong Lewis base sites coupled with nearby Lewis acid sites.

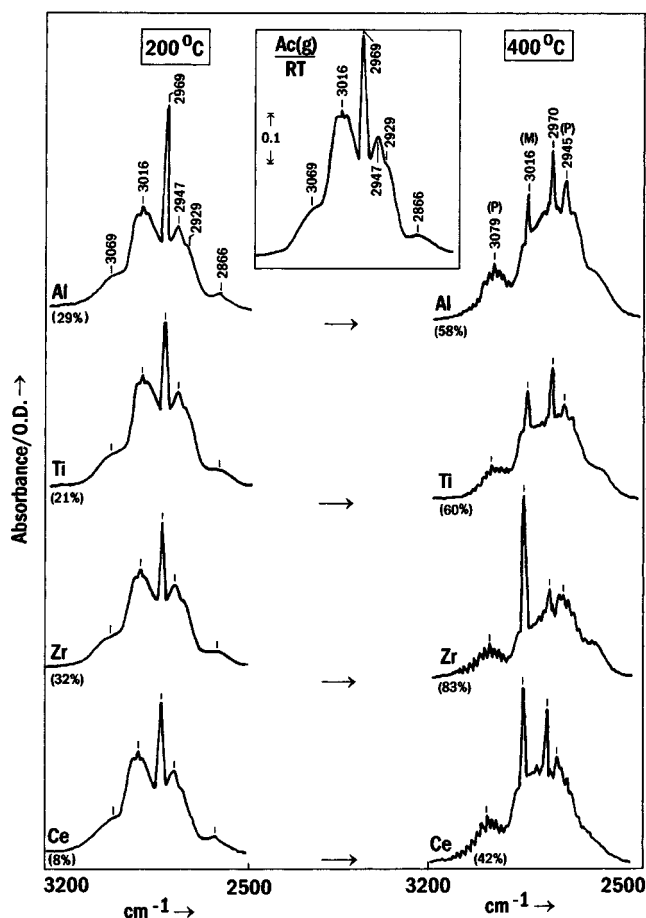


Figure 6. IR νCH gas-phase spectra recorded at RT following heating acetone vapor to 200 and 400 °C in presence of the oxides indicated. The inset displays the spectrum obtained at RT, and the parenthesized percentages are of the corresponding conversion (consumption) of acetone molecules in the gas phase. M is for methane, and P is for propene.

This is implied by the high-temperature oxidation of $\text{Py} \rightarrow \text{L}$ species into α -pyridone and pyridinium oxide species (Table 1).

Within the above context, it is interesting to recall that acetone produced during catalytic dehydrogenation of 2-propanol on $\text{Ce}^{11,34}$ (as well as on Ti and Zr)¹² is completely converted at > 200 °C into condensation gas-phase product (isobutene) and surface acetates. In contrast, acetone produced via catalytic decomposition of methylbutynol ($(\text{CH}_3)_2\text{C}(\text{OH})\text{C}\equiv\text{CH}$) on Y/MgO surfaces remains largely unchanged even at high temperatures.^{3,9} In the latter case, availability of Lewis acid–base site-pairs on Y/MgO has been considered^{3,9} to facilitate strong adsorption of condensation products of acetone (MSO), leading eventually to blockage of the catalytically active sites for Ac condensation reactions. Accordingly, the 2-propanol/Ce results may be attributed to involvement of Lewis acid sites in bonding 2-propanol adsorbed species (isopropoxide species),^{11,34} thus depriving the surface of the acid–base site-pairs necessary for strong adsorption of Ac surface species. Hence, catalytically active sites for Ac condensation reactions remain accessible.

Conclusions

The above presented and discussed results of in situ IR spectroscopy of acetone (Ac) adsorption and surface reactions on alumina (Al), titania (Ti), zirconia (Zr), and

(32) Hasan, M. A.; Zaki, M. I.; Pasupulety, L. *Proceedings of the 2nd Taylor Conference*, Liverpool University, U.K., Sept 3–7, 2000.

(33) Pierson, R. H.; Fletcher, A. N.; St. Clair Gantz, E. *Anal. Chem.* **1956**, *28*, 1218.

(34) Zaki, M. I.; Sheppard, N. *J. Catal.* **1983**, *80*, 114.

ceria (Ce) may help in drawing the following conclusions regarding the impacts of the surface acid–base properties on Ac adsorptive and catalytic interactions.

Acetone Adsorptive Interactions. The primary adsorptive interactions at Ac/oxide interfaces lead to coordination of acetone molecules to Lewis acid sites ($\text{Ac} \rightarrow \text{L}$). This type of species is stabilized at RT on surfaces that are essentially acidic and do not contain strong Lewis base sites (case of Zr, Table 1). When strong Lewis base sites are available (case of the other test oxides, Table 1), an aldol-condensation-type of reaction course (Figure 2A) is activated at RT, converting the primary $\text{Ac} \rightarrow \text{L}$ species into mesityl oxide (MSO) surface species via enolate (ENOL) and diacetone alcohol (DAA) intermediate species. Application of high temperatures up to 200 °C enhances the Ac condensation reactions on all test surfaces, but MSO is rendered the dominant surface species only on strongly basic surfaces (case of Ce, Table 1). A further increase of the temperature up to 400 °C activates surface oxidative reactions leading to conversion of Ac adsorbed species into acetate surface species and CH_4 gas phase. In such oxidative reactions, basic sites are considered to play a key role.¹⁷ When the basic sites are coupled with nearby Lewis acid sites, strong adsorption of Ac condensation products is facilitated (case of Ce, Table 1).

Acetone Catalytic Interactions. Availability of Lewis acid sites is essential for formation of the primary

$\text{Ac} \rightarrow \text{L}$ species, whereas availability of strong basic sites is important for the condensation of these primary species into DAA and MSO (Figure 2A). On the other hand, an intimate coupling between the Lewis acid and base sites generates site-pairs functioning in a concerted fashion to stabilize the Ac condensation products on the surface. Hence, catalytic active sites for Ac condensation reactions are blocked, and both adsorptive and catalytic interactions of acetone molecules are largely suppressed. This environment is well represented on Ce surfaces.

Thus, results of the present investigation suggest, in line with previous investigations,^{3,9} that C–H bond activation steps required for condensation reactions on basic oxides (typically MgO) also require cationic metal centers to stabilize carbanionic intermediates. Although coordinatively unsaturated Mg cations can play this role in MgO,^{3,9} the present results suggest that oxides of more reducible or accessible cations (i.e., CeO_2) would have Lewis acid sites of higher density and strength.

Acknowledgment. Kuwait University Research Administration Grant No. SC095 and the excellent technical support found at Analab/SAF of the Faculty of Science are highly appreciated.

LA000976P